Article

Identification of Potential Human Ryanodine Receptor 1 Agonists and Molecular Mechanisms of Natural Small-Molecule Phenols as Anxiolytics

Yahong Chen, Xiaohong Wang, Haifeng Zhai, Yanling Zhang, and Jianmei Huang*

Read Online

ACCESS | Metrics & More | Article Recommendations | Supporting Information

ABSTRACT: Natural small-molecule phenols (NSMPs) possess certain ubiquitous bioactivities including the anxiolytic effect. Ryanodine receptor 1 (RyR1) may be one of the potentially critical pharmacological targets for studying the anxiolytic activity of NSMPs. However, detailed molecular mechanisms of NSMPs have not been fully clarified. This research was intended to identify potent hRyR1 agonists from NSMPs and investigate whether RyR1 plays a role in their anxiolytic effect. Homology modeling and molecular docking analysis were performed using Accelrys Discovery Studio 2.5. The most appropriate concentrations of NSMPs to activate RyR1 were measured using the MTT assay. Fluorescence analyses of the intracellular calcium levels and western blotting analysis were carried out to validate whether NSMPs could regulate the calcium flux to some extent by activating RyR1. The results demonstrated that xanthotoxol and 5-hydroxy-1,4-naphthalenedione can be screened as hit compounds for potential agonists of hRyR1 to exert the anxiolytic effect. In conclusion, NSMPs might be a kind of pharmacological signal carrier, acting on RyR1 as an agonist and resulting in calcium ion mobilization from intracellular calcium ion store.
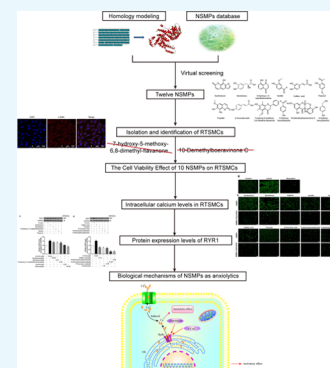
1. INTRODUCTION

Anxiety disorder, also known as anxiety neurosis, is a pervasive emotional psychiatric disorder with a morbidity of 18.10% and a lifetime prevalence of 28.80%.[1] There are mental emotions such as nervousness, panic, anxiety, irritability, and so forth, which are not commensurate with the actual environment as the main clinical manifestations.[2] One of the most widespread anxiolytic drugs prescribed for the treatment of anxiety disorders is benzodiazepines, which relieve anxiety through reinforcing activities of GABAergic by binding with the GABA$_A$ receptor complex.[3] Unfortunately, there still exists a plethora of adverse reactions such as the amnestic effect, myorelaxation, sedation, withdrawal symptoms, and so forth. Although there are some selective serotonin reuptake inhibitors, which are gradually viewed as first-line regimens for anxiety in recent decades, there are also drawbacks, especially a slower onset of therapeutic action than that of the former.[4] Therefore, it is critical to search for robust anxiolytic compounds that have more prominent antianxiety-like efficacy but fewer untoward effects. Recently, it has been reported that natural compounds from herbal medicines for treating anxiety, which are not only utilized as pharmacological tools but also are potential lead compounds for medical research and development, have a promising future.[5]

Natural small-molecule phenols (NSMPs) that originate from natural plant sources particularly refer to this kind of compound with a total molecular mass less than 350 Da and composed of three elements, carbon, hydrogen, and oxygen.[6] In particular, the common features in NSMPs' structures are at least one hydroxyl group (Figure 1). It has been reported that flavonoids significantly exerted effects on the central nervous system
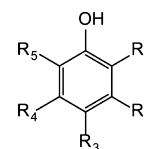
Figure 1. Chemical structure of NSMPs.

(CNS), whereas what played a crucial role in this process was their degradation products, namely, small-molecule phenols.[7] At the same time, there are numerous bioactivities of NSMPs including antianxiety,[8,9] sedation,[10,11] antispasmodic,[12,13] muscle-relaxant,[14] antioxidative,[15] neuroprotective,[16] antimicrobial,[17] and so forth. Recently, great efforts in our group have been expended to propose an unprecedented concept, "phenolism", to elucidate these common properties of NSMPs and to verify the prior hypothesis: "Anxiolytic bioactivity is one of the mutual biological activities of NSMPs".[6] Based on their

Figure 2. Information on homology modeling for hRyR1. (A) Sequence analysis of human (top) and *Oryctolagus cuniculus* RyR1 (bottom). (B) Ramachandran plot results of hRyR1. (C) Crystal structure of the central domain of hRyR1.

skeletal framework, they were divided into four categories, phenanthrenes, flavonoids, phenylpropanoids, and other phenols, to name but a few. All of them that possess extensive medical uses are regarded as pivotal components of the human diet. Therefore, NSMPs are of great importance to human health.

At present, it appears that there is no comprehensive report on the mechanism of the anxiolytic effect of NSMPs. With regard to the mechanism of known antianxiety drugs, there are mainly the neurotransmitter hypothesis, neuroendocrine dysfunction hypothesis, immune hypothesis, and so on. Currently, our main focus of the mechanism of the anxiolytic effect of NSMPs is on the neurotransmitter hypothesis.

Ryanodine receptors (i.e., RyRs), which have been considered as the largest intracellular calcium ion release channels known to date, located in the sarcoplasmic reticulum/endoplasmic reticulum (SR/ER), are necessary for calcium ion release from

intracellular stores to the cytoplasm.[18] They are homotetramers with each monomer containing nearly 5000 amino acid residues. There exist three isoforms of RyRs in the mammalian, where RyR1 is mainly expressed in the skeletal muscles, RyR2 is the predominant isoform in the cardiac muscles, and RyR3 is initially identified in the brain.[19] RyRs resemble a mushroom, and two parts constitute the giant structure, that is, a larger cap accounting for 80% of the structure is composed of the cytoplasmic region and the transmembrane region that accounts for the remaining 20% constitutes the smaller stem.[20] With the advent of the cryoelectron microscopy approach, nine diverse regions in the cytoplasmic region were reported that include the central domain (residues 3668−4251), the N-terminal domain, the handle domain, the helical domain, three SPRY domains, as well as the P1/P2 domain.[21]

Due to the enormous size of the cytoplasmic region, there is an array of binding sites for regulators of channel activity

Table 1. Information Sheet of the RyR1 Agonist 4-CmC Derivative

compound	R1	R2	R3	R4	EC$_{50}$ (μmol/L)	$-$Lg(EC$_{50}$) μmol/L	docking score
1	OH	CF$_3$	Cl	H	33.1	-1.52	69.3050
2	OH	CH$_2$CH$_3$	Cl	H	85.1	-1.93	65.4389
3	OH	CH$_3$	Br	H	110	-2.04	60.2752
4	OH	CH$_3$	CH(CH$_3$)$_2$	H	44.7	-1.65	70.5702
5	OH	CF$_3$	H	CF$_3$	30.9	-1.49	70.8800
6	OH	H	CH(CH$_3$)$_2$	H	64.6	-1.81	65.5890
7	OH	CH$_3$	Cl	CH$_3$	63.1	-1.80	63.7150
8	OH	CH$_3$	Br	CH$_3$	42.7	-1.63	63.5577
9	OH	CH$_3$	Cl	H	129	-2.11	60.3274
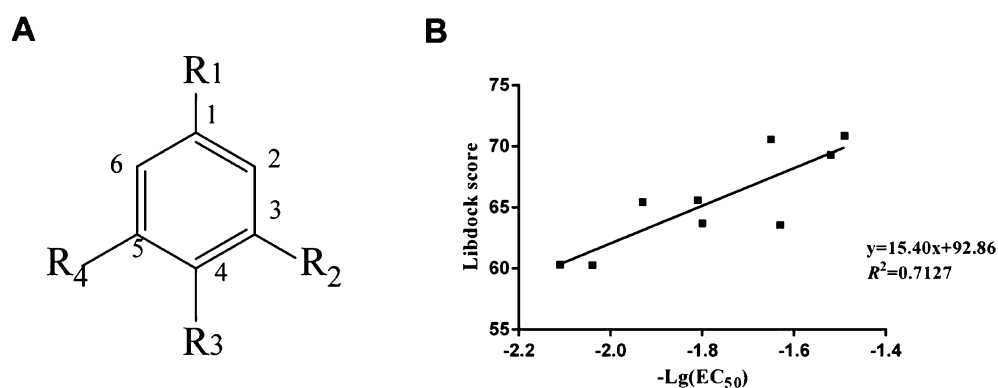
Figure 3. (A) Chemical structures of nine RyR1 agonists and (B) correlation between the Libdock score and $-$log EC$_{50}$ from in vivo biological tests.

comprising small molecules, proteins along with post-translational modifications, and so forth.[22] Notably, 4-chloro-3-methyl phenol (4-CmC), as a small molecule phenol, is a potent and specific agonist of RyR1.[23] Furthermore, Fessenden et al. elucidated that residue Gln4020 and Lys4021 of RyR1 were responsible for channel activation by 4-CmC.[24] The results showed that two amino acid residues of rabbit RyR1 (Gln4020 and Lys4021) are required for 4-CmC activation. Of these two residues, Gln4020 appears to be more important in the channel function because mutation of this residue in RyR1 results in repetitive Ca^{2+} oscillations evoked by caffeine or 4-CmC. Based on the anxiolytic effect of NSMPs, Peter Szentesi et al. indicated that thymol induced intracellular calcium release through acting directly on RyR in the mammalian skeletal muscle.[25] Sárközi et al. disclosed that carvacrol could activate RyR1 at a suitable concentration.[26] Furthermore, Lee et al. elucidated that quercetin could also increase the calcium ion release, the open probability of RyRs, and so forth.[27] An abundance of preliminary research work demonstrated that NSMPs may elicit their anxiolytic effects by affecting the release of neurotransmitters in the intercellular substances.[28,29] From this perspective, RyR1 may be one of the potentially critical pharmacologic targets for studying the bioactivities and more detailed mechanisms of NSMPs.

Owing to the structural variety of small molecules, it is unlikely that all of them induced calcium ion release through the same pathway. Additionally, the differential affinity of the small molecules that bind to the cytoplasmic region probably affects the ability of opening or closing the channel. However, the potential anxiolytic NSMPs bind to RyR1, and the molecular mechanisms for the anxiolytic effect of NSMPs are still under exploration.

Hence, the present study intends to identify the potent human ryanodine receptor 1 (hRyR1) agonists from NSMPs by means of comparing the binding affinities and binding modes between

NSMPs and hRyR1. First, 132 NSMPs were collected according to their representative pharmacological activities via SciFinder Scholar. In addition, homology modeling together with molecular docking analysis were utilized to predict potential NSMPs interacting with hRyR1. We further measured the changes in the fluorescence intensity of calcium ions in the cytoplasm and analyzed the expression of RyR1 to investigate whether RyR1 plays a role in the anxiolytic effect of NSMPs. Finally, xanthotoxol and 5-hydroxy-1,4-naphthalenedione were screened as the hit compounds for potential agonists of hRyR1 to exert an anxiolytic effect. It is noteworthy to systematically study the importance of NSMPs to human health as they are widespread in herbal medicines and diverse foods. These observations could provide profoundly new insights into predicting the bioactivities and more detailed mechanisms of NSMPs in the not too distant future.

2. RESULTS AND DISCUSSION

2.1. Homology Modeling Studies. For the RyR family, only the crystal structure of RyR1 originating from *Oryctolagus cuniculus* has been resolved. Meanwhile, the key residue of RyR1, residue Gln 4020, activated by 4-CmC is distributed in the central domain (residues 3668−4251). Therefore, the central domain of the A chain in RyR1 was constructed by homology modeling via the MODELLER program.

First, the crystal structure of RyR1 (PDB ID: 5J8V, resolution: 4.2 Å) was chosen as the template protein for homology modeling through the MODELLER program due to its highest sequence identity score (98.50%). Furthermore, the homology modeling was performed with loop and side-chain refinement. Finally, the reliability of models was evaluated using the Ramachandran plot and ERRAT. The consequences of the Ramachandran plot indicate that the residues in the core and allowable regions accounted for 96.02%. With regard to the

Table 2. Receptor−Ligand Interactions of 12 Hit NSMPs

compound	Libdock score	receptor−ligand hydrogen bonds			hydrophobic group
		atom in ligand	atom in amino acid	bond length/Å	
xanthotoxol	80.8809	O4	Gln4020 HE21	1.68	Met4000, Leu4013, Leu4016, Leu4017, Phe4061, Phe4132, Pro4135, Ala4136
		O4	Leu4017 HA	3.09	
		O1	Ala4136 HA	2.71	
		H20	Phe4132 O	2.30	
danshensu	80.6537	O3	Gln4020 HE21	1.96	Leu4013, Leu4017
		O5	Ala4136 HA	2.62	
5-hydroxy-1,4-naphthalenedione	76.5433	O12	Gln4020 HE21	2.48	Met4000, Ala4004, Leu4013, Leu4017, Phe4061, Ile4139
		H19	Phe4132 O	2.97	
		O11	Ala4136 HA	2.15	
vanillin	75.5962	O3	Gln4020 HE21	2.45	Met4000, Leu4013, Leu4017, Phe4062, Ala4136, Ile4139
		H12	Phe4132 O	2.83	
paeonol	75.0232	O3	Gln4020 HE21	2.50	Met4000, Leu4013, Leu4017, Ala4136
		O3	Leu4017 HA	2.93	
		O1	Ala4136 HA	3.04	
		H22	Phe4132 O	2.74	
caffeic acid	74.4146	O1	Gln4020HE22	2.18	Met4000, Leu4013, Leu4017, Ile4139
		O4	Phe4062 HA	2.53	
fraxetin	73.5211	O4	Gln4020 HE21	2.60	Met4000, Leu4013, Leu4017, Phe4061, Ala4136
p-coumaric acid	71.1161	O3	Gln4020 HE21	1.88	Phe4061, Pro4135, Ala4136
		H14	Leu4013 O	2.44	
7-hydroxy-5-methoxy-6,8-dimethyl-flavanone	70.7584	H29	Gln4020 OE1	1.92	Leu3993, Phe3996, Val4024, Ile4058, Phe4062, Ile4139, Val4143, Leu4146
4-hydroxybenzaldehyde	66.3870	O2	Gln4020 HE21	2.43	Met4000, Leu4013, Leu4017, Phe4062, Ala4136
		O2	Leu4017 HA	2.95	
10-demethylboeravinone C	65.0960	H28	Gln4020 OE1	1.61	Leu3993, Val4024, Ile4058, Phe4062, Val4143, Leu4146
		O23	Phe4062	2.61	
4-hydroxybenzylalcohol	64.8489	O1	Gln4020 HE21	2.44	Met4000, Leu4013, Leu4017, Phe4062, Pro4135, Ala4136

ERRAT score, overall quality factors are 90.927 greater than 80. Both of the results demonstrate that the homology modeling can be applied for subsequent studies. The homology modeling as well as the Ramachandran plot are summarized in Figure 2.

2.2. Molecular Docking Analysis. *2.2.1. Parameter Setting for Molecule Docking.* Docking parameters that play a critical role in virtual screening should be given priority for optimization. The crystal structure of 4-CmC was chosen as the reference compound. Nine agonists of RyR1 were docked to the predicted model. It turns out that Libdock scores are basically consistent with the experimental EC_{50} values, which are converted into the negative logarithmic forms.[30] Correlation analysis between the scoring function of Libdock and the experimentally measured agonists' bioactivity is carried out to elucidate the reliability of hRyR1 to identify the substrate. Finally, the docking results present similar trends to those of the in vitro study. Meanwhile, the correlation coefficient (R^2) between the Libdock score and −Log EC_{50} is 0.7127, indicating that the homology modeling has great robustness, and the docking parameters are reasonable. The docking program, Libdock, to some extent, could distinguish compounds with diverse bioactivities, which was used to predict the binding affinities between NSMPs and hRyR1 in this research. The chemical structure of nine agonists of RyR1, docking score, and the correlation between the Libdock score and −log EC_{50} are shown in Table 1 and Figure 3.

2.2.2. Virtual Screening Research. In order to discover some potent agonists of hRyR1 and the probable binding modes between ligands and receptors, virtual screening was executed

on the active site as mentioned above in this study. Prior to docking, 132 NSMPs were classified based on their mother nucleus structure and bioactivities, respectively. The specific composition information is shown in Figure S1. Then, they were docked to the binding site of hRyR1 in silico. Next, 109 top-ranking NSMPs were sifted out owing to their high Libdock scores, which were further used to observe the binding conformations and interactions with the active site, in particular, hydrogen bond interactions with the residue Gln4020. A higher Libdock score gained during the docking process manifested a stronger binding affinity between NSMPs and hRyR1. Eventually, 12 best hit NSMPs selected from top-ranking compounds are likely to be deemed as the agonists of hRyR1. The results of docking scores and the ligand−receptor interaction details are summarized in Table 2.

2.2.3. Analysis of Protein−Ligand Interactions. In this study, hydrogen bond interactions, hydrophobic interactions, and Libdock scores were recognized as the final criteria together. The chemical structures of 12 potential agonists of hRyR1 are displayed in Figure 4A. Furthermore, the binding modes of 4-CmC and 12 final hits are mapped out in Figure 4B−E. Figure 4B indicates the binding mode of 4-CmC with a Libdock score of 57.573. It has formed one hydrogen bond interaction between the hydroxyl of 4-CmC and the critical residue Gln4020, and hydrophobic interactions with Leu4013/4017, Phe4061/4062/4132, Pro4135, Ala4136, and Ile4139, as well as one pi−sulfur interaction with Met4000.

As shown in Figure 4C1, the Libdock score of xanthotoxol is 80.8809. In addition, its binding mode in the active site
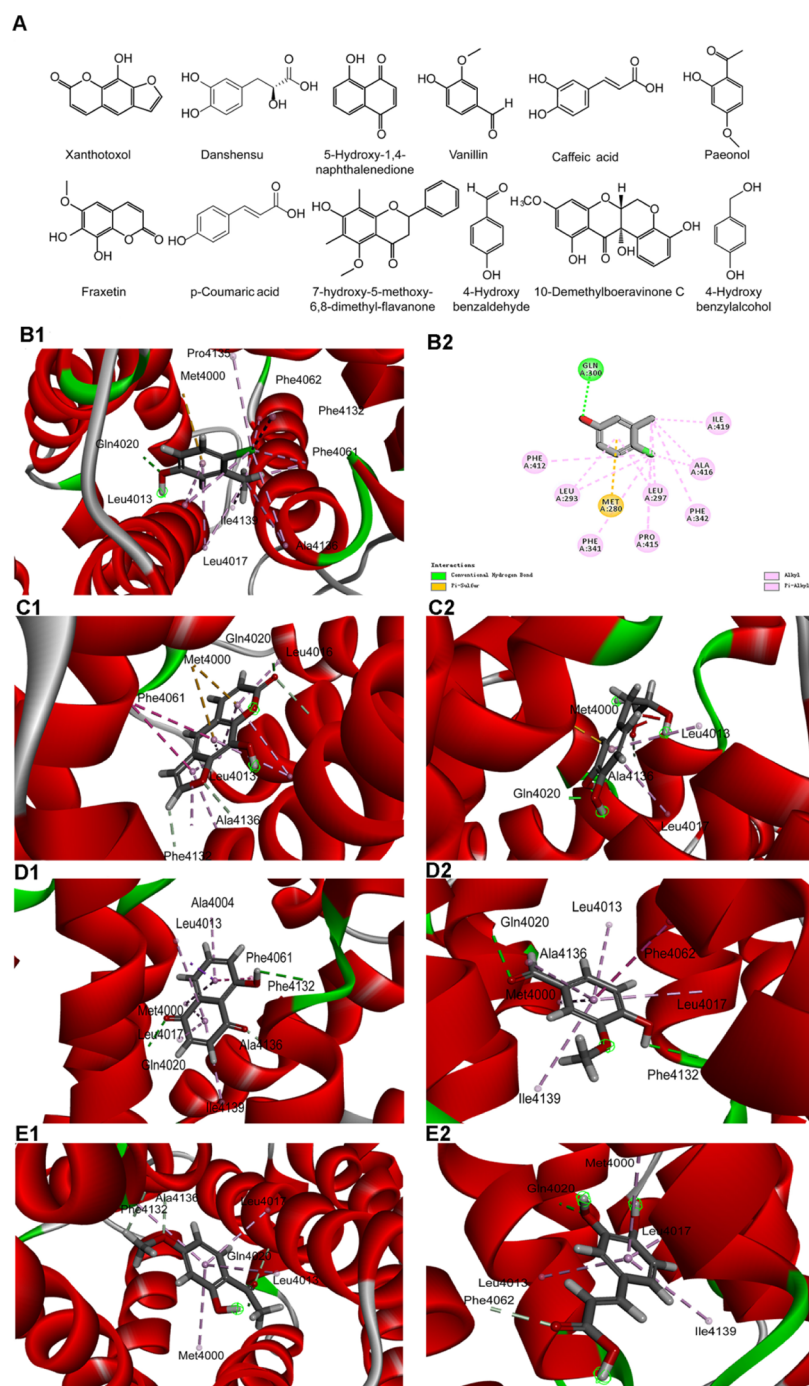
Figure 4. Docking modes between potential agonists of hRyR1 and hRyR1. Note: (A) chemical structures of 12 potential agonists of hRyR1. (B1–B2) 4-CmC, the reference small molecule, penetrated into the active pocket, and mainly formed one hydrogen bond with the Gln4020 residue on the protein, a total of nine residues were bound by the hydrophobic interaction on the hRyR1. (C1) Xanthotoxol small molecule completely penetrated the active pocket, forming four hydrogen bonds with the Gln4020, Leu4017, Phe4132, and Ala4136 residues on the protein. The hydrophobic interaction residues of the xanthotoxol molecule were eight. (C2) Danshensu molecule completely enters the active pocket, Gln4020 and Ala4136 residues form two hydrogen bonds with a total of two hydrophobic residues. (D1) 5-Hydroxy-1,4-naphthalenedione (i.e., juglone) small molecule enters the active pocket, forming three hydrogen bonds with Gln4020, Phe4132, and Ala4136, and six residues form exhibiting a hydrophobic effect. (D2) Vanillin completely enters the active pocket and forms a hydrophobic interaction with six residues. (E1) The paeonol molecule completely penetrates the active pocket, forming four hydrogen bonds with Gln4020, Leu4017, Phe4132, Ala4136, and a total of four hydrophobic residues. (E2) Caffeic acid completely enters the active pocket, and four residues form a hydrophobic effect.

resembled 4-CmC. Xanthotoxol could form a conventional hydrogen bond interaction with Gln4020 and carbon–hydrogen bond interactions with Leu4017, Phe4132, and Ala4136, respectively. Moreover, xanthotoxol participates in van der Waals interactions with Phe4062, Ile4139, and other residues.

The binding mode of the xanthotoxol–hRyR1 complex is stabilized by pi–pi and pi–alkyl interactions and four hydrophobic residues. Furthermore, Met4000 is involved in the pi–sulfur interactions.
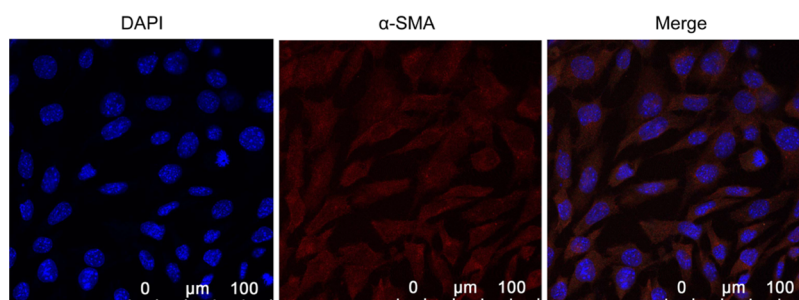
Figure 5. Positive results of identification on RTSMCs. The expression level of α-SMA was detected using immunofluorescent staining analysis by confocal microscopy. Blue fluorescence indicates DAPI labeled nuclei, and red fluorescence represents α-SMA positive expression. Scale bar, 100 μm.

Like 4-CmC, danshensu has formed a conventional hydrogen bond with Gln4020 and a carbon–hydrogen bond with Ala4136, which plays important roles in activating calcium channels. Other interactions involved in danshensu are pi–alkyl and pi–sulfur interactions (Figure 4C2).

5-Hydroxy-1,4-naphthalenedione could form the same hydrogen bond type as 4-CmC with Gln4020. In addition, Phe4132 and Ala4136 are also involved in hydrogen bond interactions. 5-Hydroxy-1,4-naphthalenedione interacts by means of van der Waals interactions with Phe4062, Pro4135, and other residues. The receptor–ligand complex remains stable through six hydrophobic interaction residues and three types of pi bonds (Figure 4D1).

Vanillin could participate in hydrogen bond interactions with Gln4020 and Phe4132. The docked conformation of vanillin is comparable to that of 4-CmC. Both of them interact with hRyR1 via more hydrophobic interactions, whereas vanillin forms by van der Waals interactions (Figure 4D2).

The binding mode of paeonol with a Libdock score of 75.0232 is displayed in Figure 4E1. It has formed three carbon–hydrogen bonds with Leu4017, Phe4132, and Ala4136 as well as one conventional hydrogen bond with Gln4020. Besides the fact that the interactions that occur between paeonol and hRyR1 are van der Waals interactions, with Phe4062, Ile4139, and other residues, there exist an array of pi–alkyl interactions.

As illustrated in Figure 4E2, caffeic acid participates in hydrogen bond interactions with the critical residue Gln4020 and forms a carbon–hydrogen bond with Phe4062. Leu4017 and Pro4135 are concerned with pi–alkyl interactions and van der Waals interacting forces, respectively.

Overall, our docking results reveal that all the 12 NSMPs possess higher docking scores than 4-CmC. The high Libdock scores gained in this study validate that there exist a stronger binding affinity between the 12 NSMPs and hRyR1. Hydrogen bonds and hydrophobic interactions formed between the agonists and the essential active site residues might be responsible for it. A visualization of potential binding orientations exhibits the hydrogen bond interactions with the critical residue Gln4020 and hydrophobic interactions with Met4000, Phe4061, Phe4062, Leu4013, Leu4017, Ala4136, and Ile4139. It has been reported that Gln4020 plays pivotal roles in the channel function on account of the fact that repetitive calcium oscillations triggered by 4-CmC occurred when this residue in RyR1 was mutated. Thus, these interactions of 12 NSMPs with hRyR1 demonstrate that there is a good complex at the ligand domain of hRyR1. The specific composition information is shown in Figure S2. Moreover, these 12 potential agonists on further optimization could be utilized for designing novel hRyR1 agonists.

2.3. Isolation and Identification of Rabbits' Tracheal Smooth Muscle Cells. In this study, the cell type that was obtained by the acute pronase separation method is single, easy to distinguish, and in large quantities. In addition, the cell morphology is diverse, particularly more common in the shape of earthworm and banana, accounting for 70−80%. Others have oval, circle, and irregular shapes. The cells vary in size from 12 to 16 μm in diameter and approximately from 60 to 100 μm in length. The cell structure is clearly viewed, possessing smooth membrane surfaces, as well as few intracellular particles. The immunofluorescence staining results indicate that the positive rate of rabbits tracheal smooth muscle cells (RTSMCs) accounted for up to 90%, thus they could be used in later cell experiments. This technique stains the α-SMA characteristic of smooth muscles, producing a red color, and DAPI staining generated a blue color for the α-SMA nuclei (Figure 5).

2.4. Cell Viability Effect of NSMPs on RTSMCs. Because 2 of 12 NSMPs, which may become potential hRyR1 agonists, that is, 10-demethylboeravinone C and 7-hydroxy-5-methoxy-6,8-dimethyl-flavanone, were not available, a further study was performed on the remaining 10 NSMPs. For the sake of selecting the most appropriate concentrations of NSMPs to activate RyR1 in subsequent experiments, the cell proliferation activity of NSMPs (0.016, 0.16, 0.8, 1.6, 3.2, 8.0, 16.0, and 32.0 μM) on RTSMCs was measured by 3-(4,5-dimethylthiazol-2-yl)-2,5-diphenyltetrazolium bromide (MTT) detection, and the IC_{50} value was used as an evaluation indicator. The results of the MTT assay showed that compared with the control group, the cell proliferation activity of different concentrations of the NSMP group decreased ($P < 0.001$, $P < 0.0001$). The cell proliferation activity of the NSMP group was dose-dependent (Figure 6A−J). Therefore, and for the next protocol, we chose concentration levels of xanthotoxol of 28.29 μM, danshensu of 2.57 μM, 5-hydroxy-1,4-naphthalenedione (i.e., juglone) of 0.38 μM, vanillin of 0.98 μM, paeonol of 29.46 μM, caffeic acid of 6.15 μM, fraxetin of 1.78 μM, p-coumaric acid of 3.90 μM, 4-hydroxybenzaldehyde of 14.48 μM, and 4-hydroxybenzylalcohol of 9.44 μM. The specific composition information is shown in Figure S3 and Table S1.

2.5. Effects of NSMPs on Intracellular Calcium Levels in RTSMCs. Calcium ions, intracellular signal molecules, used as a second messenger in the cells, are essential for the process of signal transduction. In order to find out whether NSMPs could regulate the change of calcium flux by stimulating RyR1, we further assayed the intracellular calcium levels in RTSMCs after treating with 10 NSMPs mentioned above. As shown in Figure 7A−J, when compared with the non-treated control, the levels of intracellular calcium were significantly elevated in cells of the groups treated with xanthotoxol, danshensu, 5-hydroxy-1,4-
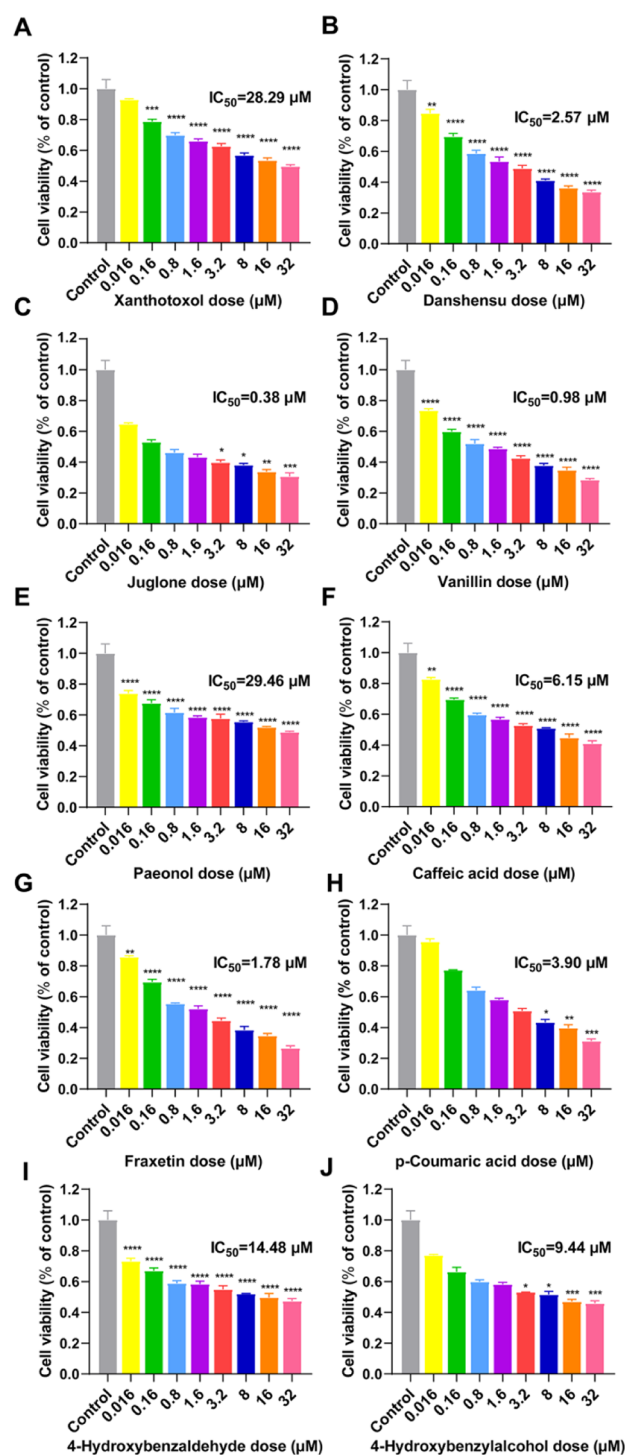
Figure 6. Effects of 10 NSMPs on the viability of RTSMCs. The cell viability of RTSMCs treated with (A−J) xanthotoxol (28.29 μM), danshensu (2.57 μM), 5-hydroxy-1,4-naphthalenedione (i.e., juglone, 0.38 μM), vanillin (0.98 μM), paeonol (29.46 μM), caffeic acid (6.15 μM), fraxetin (1.78 μM), p-coumaric acid (3.90 μM), 4-hydroxybenzaldehyde (14.48 μM), and 4-hydroxybenzylalcohol (9.44 μM) was determined by the MTT assay. The results are treatment group means, and vertical lines represent SD. Significant differences from the control group are denoted by *P < 0.05, **P < 0.01, ***P < 0.001, and ****P < 0.0001. Differences were assessed for significance by Dunnett's T3 multiple comparisons test subsequent to significant one-way ANOVA.
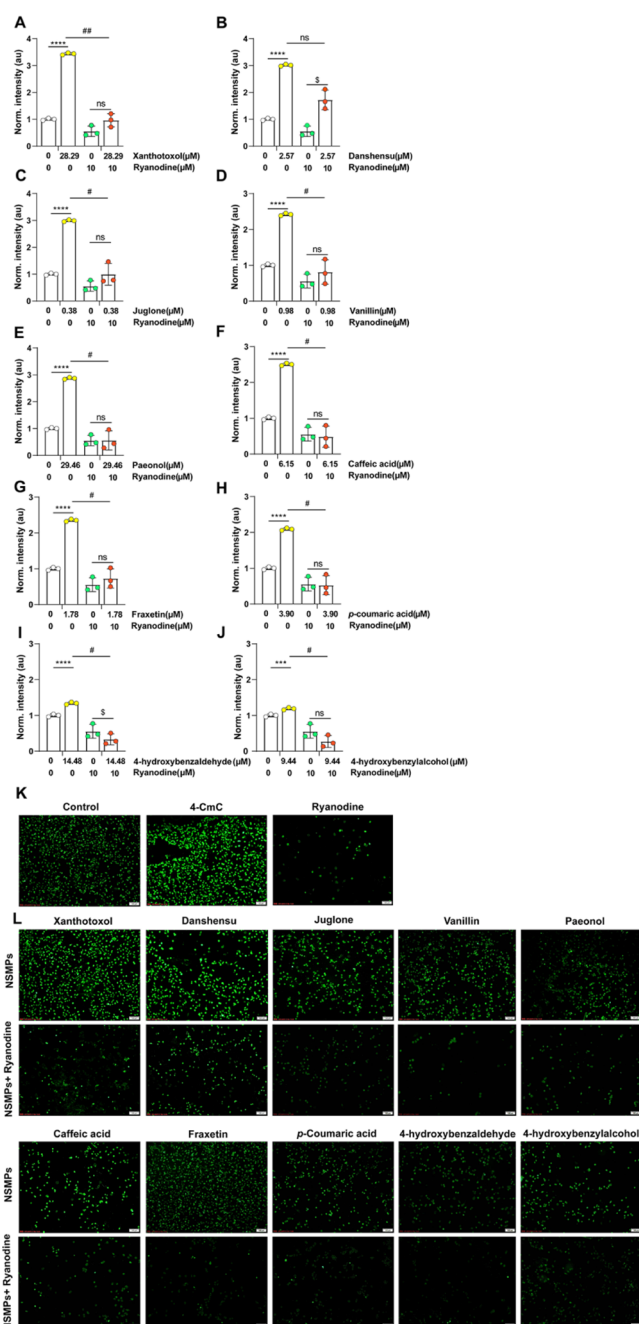
Figure 7. Effect of 10 NSMPs on intracellular calcium levels in RTSMCs. (A−J) Normalized fluorescence intensity was calculated by the average intensity of each group, and then it was normalized to divide the average intensity of the treatment group by the average intensity of the vehicle group. The results are the treatment group means, and vertical lines represent SD. Significant differences from the vehicle/vehicle-treated group are denoted by ***P < 0.001, ****P < 0.0001. Significant differences to the NSMP/vehicle-treated group are denoted by #P < 0.05, ##P < 0.01. Significant differences to the vehicle/ryanodine-treated group are denoted by $P < 0.05. (K,L) Fluo-4 AM-labeled RTSMCs with intervention from ryanodine (10 μM), 4-CmC, and NSMPs. Scale bars: 100 μm (K,L). For all figures: two-way ANOVA; ns, no significant difference; and n = 3 biologically independent samples.

naphthalenedione, vanillin, paeonol, caffeic acid, fraxetin, p-coumaric acid, 4-hydroxybenzaldehyde, and 4-hydroxybenzylalcohol (P < 0.001, P < 0.0001). The intracellular calcium
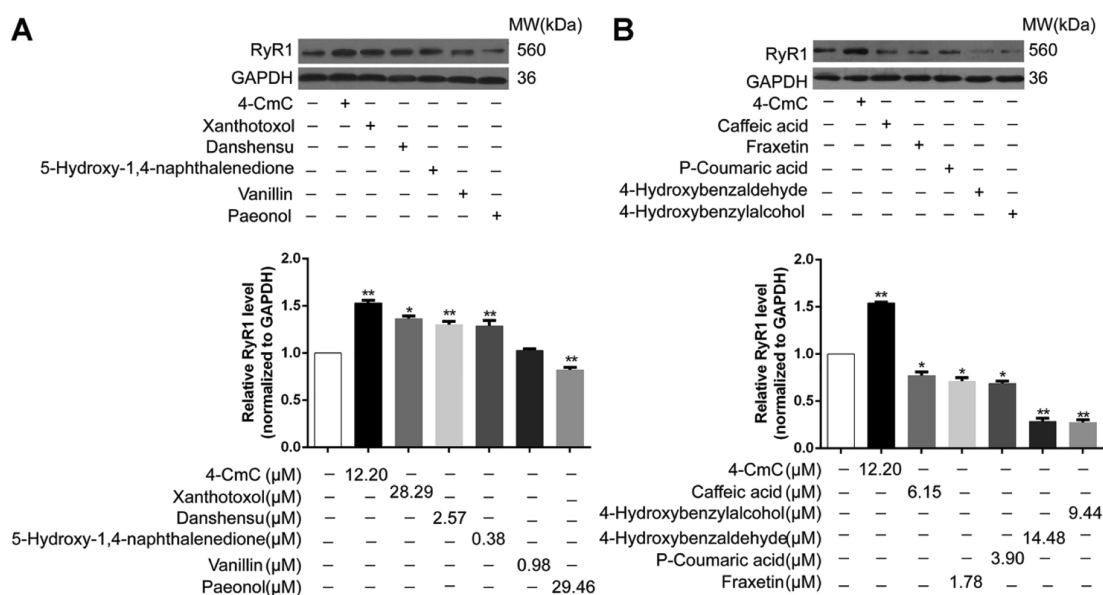
Figure 8. Effect of 10 NSMPs on the expression levels of RyR1 in RTSMCs. (A) After RTSMCs were treated with 4-CmC or different concentrations of NSMPs, the protein expression of RyR1 was detected by western blotting. (B) Quantitative histogram of RyR1 treated with 4-CmC or different concentrations of NSMPs. The results are the treatment group means, and vertical lines represent SD. Significant differences from the control group are denoted by *$P < 0.05$, **$P < 0.01$. Differences were assessed for significance by Dunnett's T3 multiple comparisons test subsequent to significant one-way ANOVA.

fluorescence intensity of the NSMPs + ryanodine group was significantly lower than that of the NSMPs group with corresponding concentrations ($P < 0.01$, $P < 0.05$), and there was no significant difference compared with the ryanodine group. However, the intracellular calcium fluorescence intensity of the danshensu + ryanodine group was not significantly different than that of the danshensu group. $[Ca^{2+}]_{cyt}$ in RTSMCs exposed to 4-hydroxybenzaldehyde together with ryanodine was lower than that of the ryanodine group ($P < 0.05$).

2.6. Effects of NSMPs on RyR Expression in RTSMCs. Previous results initially suggested that NSMPs could indeed act on RyRs and result in calcium ion mobilization from intracellular calcium ion store. In order to further explore whether the change of RyR1 activity was related to its protein expression level, western blotting analysis was carried out to analyze protein expression levels of RyR1. 4-CmC here was utilized as a positive control in various in vitro studies, which has been reported to strongly and specifically activate RyR1. As exhibited in Figure 8A, protein expression levels of RyR1 were significantly increased after treatment with xanthotoxol, danshensu, and 5-hydroxy-1,4-naphthalenedione, which were compared with those of the non-treated control. However, compared to the non-treated control group, with RTSMCs exposed to paeonol, caffeic acid, fraxetin, *p*-coumaric acid, 4-hydroxybenzaldehyde, and 4-hydroxybenzylalcohol, protein expression levels of RyR1 indicated a decreasing tendency as well as significant differences between the groups ($P < 0.05$). Especially, following treatment with 4-hydroxybenzaldehyde and 4-hydroxybenzylalcohol, protein levels of RyR1 were obviously reduced by approximately 3.6-fold and 3.7-fold than those in non-treated control, respectively ($P < 0.01$, Figure 8B). Overall, consistent with the above observations, RyR1 has been proved to be one of the potential targets of NSMPs, involved in the molecular mechanisms of their anxiolytic effect.

3. CONCLUSIONS

In recent decades, natural compounds extracted and isolated from traditional Chinese herbal medicines have a promising profile.[31] NSMPs, natural organic compounds, which are composed of at least one hydroxyl group, have some structural diversities. Phenols have numerous common bioactivities, such as sedation, spasmolysis, antitumor, as antioxidant, and so forth.[32] Recently, growing evidence has proved that some flavonoids reflecting anxiolytic activities have a significant role in the CNS.[33−40] Other research studies have suggested the metabolism of flavonoids into smaller-molecular-weight phenols by intestinal flora as the key to produce anxiolytic activities.[7] Thus, in this research, the hypothesis we have put forward is that NSMPs are generally anxiolytic, and a preliminary discussion was carried out to illustrate the possible molecular mechanisms of action.

Intracellular calcium, a novel second messenger, plays a crucial role in a series of cell function-based physiological processes such as muscle contraction, gene transcription, synaptic transmission, hormone secretion, programed apoptosis, and necrosis.[41] Under normal conditions, calcium release from ER/SR into the cytoplasm is mediated by two families of proteins, that is, RyRs and inositol-1,4,5-triphosphate receptors (IP$_3$Rs), which then reuptakes it back into ER/SR via the calcium pump to maintain a dynamic balance. When a cell is stimulated, Ca^{2+} concentration in a specific region of the cell increases, and the signal is transmitted throughout the cell, resulting in a cell-wide effect.[42] In addition to the excitation−contraction coupling of myocytes, RyRs play a vital role in a variety of physiological processes including cell proliferation and death during development and differentiation, signal transduction of nerve cells, and hormone secretion in the immune system. Meanwhile, intracellular small molecules, which have a significant impact on the intensity and sensitivity of calcium release and thus regulate the open and closed states of RyRs, are the basic requirement for RyR functioning.[43] 4-CmC is a simple

small-molecule phenol that is deemed a specific agonist of RyR1 to regulate calcium release in the cytoplasm.[23] However, whether NSMPs with similar structures could modulate RyR1-mediated calcium signaling remains to be explored.

In this work, the binding affinities between 132 NSMPs and hRyR1 were evaluated using the molecular docking assay. Fessenden et al. elicited that the activation of 4-CmC on RyR1 was eliminated, when Gln4020 and Lys4021 were mutated to their corresponding residues in the structure of RyR3 (Leu3873 and Gln3874), demonstrating that they were the key amino acids of RyR1. Gln4020 seems to be more important in the aspect of regulating calcium channels, which embodies that mutations in Gln4020 could repeatedly trigger calcium oscillations. Therefore, changes in the intracellular calcium concentration could be encoded into complex and diverse signals by oscillation to enable calcium to regulate numerous functions of cells specifically.[24] Based on this, the active pocket was constructed with the key amino acid Gln4020 as the center for virtual screening. In light of our docking results, xanthotoxol, danshensu, 5-hydroxy-1,4-naphthalenedione, 4-hydroxybenzaldehyde, 10-demethylboeravinone C, caffeic acid, 7-hydroxy-5-methoxy-6,8-dimethyl-flavanone, 4-hydroxybenzylalcohol, vanillin, paeonol, fraxetin, and p-coumaric acid are mainly grouped into flavonoids, phenylpropanoids, and other phenols. However, we found that phenanthrenes could also bind to the active site in the binding pocket, but they are unable to interact with all the critical residues at the binding sites. That is to say, the reason why phenanthrenes fail to interact with the active sites during our docking study is that the ligand size might play an important role in it. Meanwhile, our docking results suggest that there are two significant factors: (1) Gln4020, as a hydrophilic residue, mainly stabilizes the hydroxyl group of NSMPs through hydrogen bond interactions. (2) The hydrophobic groups on the benzene rings and the benzene ring of NSMPs itself interact with the hydrophobic surface of hRyR1. It was found that hydrophobic interactions with Met4000, Phe4061, Phe4062, Leu4013, Leu4017, Ala4136, and Ile4139 are mainly formed between NSMPs and hRyR1. Recently, an emerging body of research has shown that a wide range of compounds were equipped with the ability to activate or inhibit calcium release channels.[14,44−49] In particular, a majority of channel activators are electron acceptors, while channel inhibitors are electron donors. Ye et al. designed a series of new compounds that have been proven to be potent inhibitors of RyR1 by means of improving the electron donor properties.[50] In this study, 12 NSMPs bind to the same region of hRyR1 as 4-CmC, indicating that their bioactivity might be similar to that of 4-CmC. Furthermore, Marinov et al. have demonstrated that the effectiveness of new drugs was highly correlated with the potency of electron acceptors or donors, namely, channel activators or inhibitors.[51] Therefore, it occurred to us all whether it is possible to design potent channel agonists by enhancing the electron acceptor properties of drugs targeting hRyR1.

The MTT assay was performed to determine the appropriate concentrations of xanthotoxol, danshensu, 5-hydroxy-1,4-naphthalenedione, vanillin, paeonol, caffeic acid, fraxetin, p-coumaric acid, 4-hydroxybenzaldehyde, and 4-hydroxybenzylalcohol. The results showed that all the above NSMPs had inhibition growth effects on RTSMCs with different levels in a dose-dependent manner.

In order to further validate whether these 10 NSMPs have an agonistic effect on RyR1, fluorescence analyses of the intracellular calcium levels and western blotting analysis in RTSMCs

were performed to analyze the changes in the intracellular calcium flux and protein expression levels of RyR1. 4-CmC here was applied to be a positive control in various in vitro studies, which has been reported to strongly and specifically activate RyR1.[52] Ryanodine, which binds to the intracellular calcium channel and opens it at a low concentration ($<10\ \mu$M) while inactivates it at high concentration ($\geq 10\ \mu$M), has been proven to have a main effect on controlling the release of intracellular calcium stores.[53] The dosage of ryanodine used in this study is 10 μM, belonging to a high concentration range, and thus it blocks the release of calcium triggered by binding of ryanodine to receptors.[54] $[Ca^{2+}]_{cyt}$ in RTSMCs exposed to p-coumaric acid, xanthotoxol, danshensu, 5-hydroxy-1,4-naphthalenedione, vanillin, paeonol, caffeic acid, fraxetin, 4-hydroxybenzaldehyde, and 4-hydroxybenzylalcohol were significantly elevated. The intracellular calcium fluorescence intensity of the NSMPs + ryanodine group was significantly lower than that of the NSMP group with the corresponding concentration, and there was no significant difference compared with the ryanodine group. It was suggested that the RyR pathway was blocked by the high concentration of its blocker ryanodine, thus blocking one of the pathways for the release of calcium from ER. What is particularly noteworthy is that the intracellular calcium fluorescence intensity of the danshensu + ryanodine group was not significantly different than that of the danshensu group while higher than that of the ryanodine group, indicating that danshensu activated another pathway for intracellular calcium release, namely the IP_3 signaling pathway, when the ryanodine pathway was blocked. Moreover, $[Ca^{2+}]_{cyt}$ in RTSMCs exposed to 4-hydroxybenzaldehyde together with ryanodine was lower than that of the ryanodine group, demonstrating that in addition to the blocking of the RyR pathway, another IP_3R pathway was also blocked by adding 4-hydroxybenzaldehyde. Both the release pathways of calcium in endoplasm were blocked, so intracellular calcium ionic strength was further reduced. In other words, 4-hydroxybenzaldehyde acted on the IP_3 receptor to inhibit the release of intracellular calcium. To sum up, p-coumaric acid, xanthotoxol, 5-hydroxy-1,4-naphthalenedione, vanillin, paeonol, caffeic acid, fraxetin, and 4-hydroxybenzylalcohol might act on RyRs as agonists, keeping RyRs open and resulting in calcium ion mobilization from intracellular calcium ion store. Among them, 4-hydroxybenzaldehyde, 4-hydroxybenzylalcohol, p-coumaric acid, danshensu, paeonol, and caffeic acid, all these NSMPs have obvious anxiolytic activity. This may be due to the fact that NSMPs do not act on a single receptor. For the anxiolytic mechanism, numerous references report that NSMPs have effects on neurotransmitters and responding receptors. Kwon et al.[55] found that danshensu played an antianxiety role through the dopaminergic nervous system, which was embodied in the inhibition of monoamine oxidase A activity in vitro, and its anxiolytic activity could be antagonized by the dopamine (DA) D1 receptor antagonist, but not by the 5-HT$_{1A}$ receptor antagonist and the α_{1A} adrenergic receptor antagonist. Studies have shown that caffeic acid could indirectly regulate the α_{1A} adrenergic receptor without affecting monoamine neurotransmitter reabsorption and monoamine oxidase activity, thus exerting an antianxiety effect.[56] p-Coumaric acid and 4-hydroxybenzaldehyde played an anxiolytic role by acting on the BDZ binding site of the GABA$_A$ receptor.[57,58] The antianxiety effect of 4-hydroxybenzylalcohol, a small-molecule phenol in *Gastrodia elata*, could be blocked by the 5-HT$_{1A}$ receptor.[58] Moreover, it is possible that NSMPs act on RyR1 in different brain regions. In mammals, both RyR1 and RyR3 exist
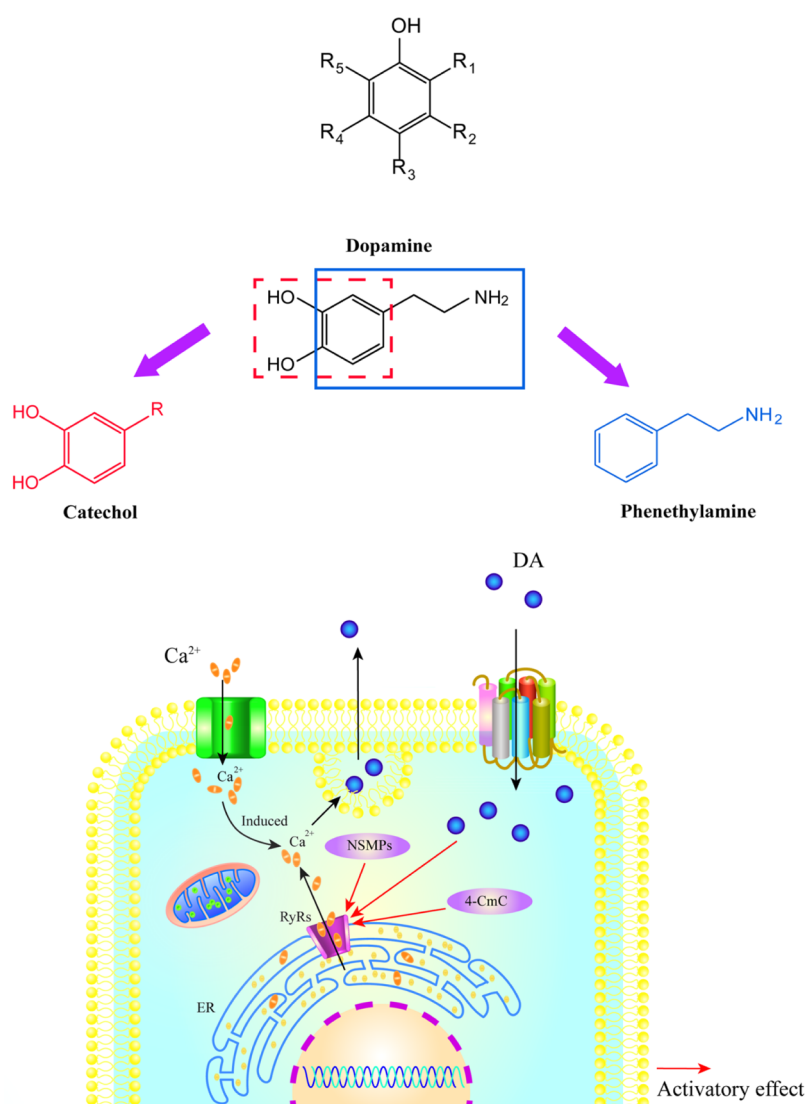
Figure 9. Hypothesis about the mechanisms of NSMPs as anxiolytics. The phenol moiety of monoamine neurotransmitters may be a kind of pharmacological signal carrier, acting on RyRs as an agonist and resulting in calcium ion mobilization from intracellular calcium ion store. Phenol keeps RyRs open, which leads to the depletion of calcium ions from ER, then the failure of calcium-induced plasmic calcium increases and finally decreases the neurotransmitter release. For all figures: NSMPs, natural small-molecule phenols; RyRs, ryanodine receptors; and ER, endoplasmic reticulum.

in skeletal muscle cells. RyR1/RyR3 or RyR2/RyR3 exists simultaneously in hippocampal CA2 and CA3 regions of the brain and neurons in the cerebellum, especially in hippocampal CA1 region neurons with high levels of expression of the three subtypes.[59]

For the sake of further exploring whether the change of RyR1 activity was related to its protein expression level, western blotting analysis was carried out to analyze protein expression levels of RyR1. As a result, the protein expression levels of RyR1 were significantly increased after treatment with xanthotoxol, danshensu, and 5-hydroxy-1,4-naphthalenedione. There was no significant change in the expression of RyR1 exposed to vanillin, while the expression levels of RyR1 exposed to paeonol, caffeic acid, fraxetin, p-coumaric acid, 4-hydroxybenzaldehyde, and 4-hydroxybenzylalcohol were significantly decreased, showing inhibitory effects on RyR1 to some extent. The possible reasons are as follows: (1) the chemical structure determines the biological activity of the compound. In the structure of vanillin, the aldehyde group at the fourth position is an electrophilic group. Based on the results of previous literature research, the

activity of small-molecule phenols could be enhanced when the fourth position is replaced by hydrophobic groups, while the activity could be decreased when the fourth position is replaced by hydrophilic groups or the electrophilic group. (2) Molecular docking methods have some limitations. First of all, the LibDock algorithm used in this study is based on the principle of semiflexible docking, so it fails to fully consider the flexibility of proteins; however, in most cases, the conformational change of biomolecular molecules is one of the important factors that induce ligands to bind to them. Second, most molecular docking procedures fail to adequately consider the effect of water molecules on hydrogen bonds during ligand binding. Therefore, molecular docking methods should be combined with biological experiments to exclude false positive results in tests.

In conclusion, the change of the RyR1 activity caused by 5-hydroxy-1,4-naphthalenedione and xanthotoxol might be due to the increased protein expression of RyR1. Based on the previous studies of our research group and multiple literature investigations,[60−65] we found that the structures of NSMPs and phenethylamines are similar to that of the monoamine

neurotransmitter, that is, DA. Through the structural comparison of three types of compounds, that is, NSMPs, DA, and phenethylamines, it is astonishing to us all to discover that the structure of DA is composed of two parts: catechol derivatives and phenethylamine derivatives. DA, an important neurotransmitter in the CNS, is mainly involved in the regulation of exercise, emotions, and the neuroendocrine system, playing a critical role in the brain and body.[61] Over the past 3 decades, the DA system has attracted much attention in the aspect of neuroscience research. Some diseases including Parkinson's disease, schizophrenia, and so on are related to the disorder of dopaminergic neurotransmitter transmission.[66,67] The phenol moiety of monoamine neurotransmitters including DA, norepinephrine, and serotonin makes a difference in the pathological process of anxiety, which may be considered as a kind of pharmacological signal carrier acting on RyRs as an agonist and resulting in calcium ion mobilization from intracellular calcium ion store. Phenol keeps RyRs open, which leads to the depletion of calcium ions from ER, then the failure of calcium-induced plasmic calcium increases and finally decreases the neurotransmitter release (Figure 9).

In the present study, it is established that 5-hydroxy-1,4-naphthalenedione and xanthotoxol might be a kind of pharmacological signal carrier, acting on RyR1 as an agonist and resulting in calcium ion mobilization from intracellular calcium ion store. This is the first time a novel insight has been gained into the idea that RyR1 may be one of the targets of NSMPs to exert an anxiolytic effect. Although more data are needed to support our hypothesis, it may provide new ideas for the rational use of herbal medicines and the development of new anxiolytic drugs.

4. MATERIALS AND METHODS

4.1. Chemicals, Antibodies, and Animals. HBSS was obtained from Kermel Chemical Co. Ltd. (Tianjin, China). DMSO was bought from Invitrogen Corporation (Waltham, MA, USA). Pronase, fetal bovine serum (FBS), Dulbecco's modified Eagle's medium (DMEM), phosphate buffered saline (PBS), and MTT were bought from GIBCO-BRL (San Francisco, CA, USA). Antibodies against α-SMA, RyR1, and GAPDH, and the antirabbit IgG horseradish peroxidase-conjugated secondary antibody were all bought from Abcam (Cambridge, UK). The fluorescence-conjugated secondary antibody was obtained from KPL Corporation (USA). The calcium ion fluorescent probe kit was obtained from Solarbio Biotechnology (Beijing, China). Ryanodine was purchased from SIGMA Corporation (USA). Xanthotoxol, danshensu, 5-hydroxy-1,4-naphthalenedione, vanillin, paeonol, caffeic acid, fraxetin, *p*-coumaric acid, 4-hydroxybenzaldehyde, and 4-hydroxybenzylalcohol were all bought from Shanghai Yuanye Biotechnology Co., Ltd. (Shanghai, China).

Healthy male and female New Zealand rabbits weighing 1.5 $\pm$ 0.3 kg were bought from the Experimental Animal Center of Hebei Medical University, and the study was approved by the Chinese Academy of Medical Sciences (certificate no. SYXK 2015-0002, Institute of Hematology and Blood Diseases Hospital, Chinese Academy of Medical Sciences and Peking Union Medical College, Tianjin, China). In this research, experimental animals were raised based on the international guidelines for laboratory animal use.

4.2. Homology Modeling Studies. The homology modeling process consisted of the following steps. First, the human RyR1 (hRyR1, NP_000531.2) was exploited as the

keyword to perform sequence similarity searches in the NCBI protein database using PSI-BLAST. The target sequence was utilized as the query to filtrate and download the most probable template proteins from the Protein Data Bank. There exist three criteria for selecting template proteins: (1) the sequence homology should be greater than 30%. (2) It is ensured that the residues are integrated. (3) The template proteins bound to have a higher precision. Furthermore, the most probable template proteins were used for building models via the MODELLER program. Subsequently, the reliability of models was evaluated by the Ramachandran plot and ERRAT. The Ramachandran plot is generally used to elucidate the allowed and disallowed conformations in the protein or peptide by comparing the rotation degree of the bond between the alpha carbon atom and the carbonyl carbon atom with the rotation degree of the bond between the alpha carbon atom and nitrogen atom in the peptide bond of the steric structure. In general, if the residues in the core and allowable regions account for more than 90%, the conformation of the predicted model is considered to be in accordance with the stereochemical rules. ERRAT is often utilized to assess the matching relationship between the predicted model and its own sequence. A higher ERRAT score represents the greater credibility of the constructed model.[68] Based on the results of the assessment, unreasonable residues in the model were executed using loop and side-chain refinement.

4.3. Molecular Docking. *4.3.1. Ligand and Protein Preparation.* In this study, the structures of NSMPs and the reference compound were collected as described previously.[6] By searching the SciFinder database, NSMPs were collected, and their chemical information was summarized, and a library of NSMP compounds was established. The specific retrieval process was as follows: (1) the chemical structure of phenol was used as the parent nucleus for "substructure" retrieval, and the molecular weight was limited to be less than 350 Da. (2) A database of NSMPs was obtained by removing the structures containing N, P, S, and other heteroatoms from the obtained compounds. (3) The related activities of "anxiolytic", "sedative", and "muscle relaxant" corresponding to NSMPs were retrieved. (4) Target compounds were screened from the collected literature.

The chemical structures of ligands were downloaded from the PubChem database together with the Traditional Chinese Medicine Database. Moreover, the Chemistry at HARvard Macromolecular Mechanics (CHARMm) force field was added to the ligands' chemical structures, and then energy minimization was implemented. Eventually, the Prepare Ligands Protocol was implemented with the following parameters: [Duplicate Structure] Remove, [Generate 3D] True, others were False.

Owing to the fact that the three-dimensional structure of hRyR1 is not available in the PDB database, it was built by homology modeling. Recently, the research team of Professor Chang-Cheng Yin and Fei Sun characterized a calcium-activated open-stated RyR1 (PDB ID: 5J8V) structure with a resolution of 4.2 Å in the core region.[69] A complete protein chain of hRyR1 contains 5037 amino acid residues. In the present study, the central domain (residues 3668−4251) of the A chain was used as the template protein for homology modeling on account of the fact that the key residue of RyR1, residue Gln 4020, activated by 4-CmC is distributed in this region. The residues 3668−4251 of the A chain in the structure of RyR1 correspond to the residues 1−500 in the structure of hRyR1, respectively. The

crystal structure of RyR1 was downloaded from the PDB database. All water molecules were gotten rid of; thereafter, polar hydrogen atoms as well as all the missing residues were added to the protein structure. Eventually, the Prepare Protein Protocol was implemented.

4.3.2. Parameter Setting for Molecular Docking. A docking program, which is utilized to forecast the binding affinity between a certain ligand and a protein, is unlikely to provide a good prediction for all the protein—ligand complexes, although in most cases an accurate and robust consequence is desired. Under this circumstance, a positive control was supposed to be set up in order to evaluate the reasonability of docking parameters by comparing the sequence between docking scores and experimental EC_{50}. Nine RyR1 agonists that have been reported for the experimental EC_{50} in the previous study were screened as the positive control. All the experimental EC_{50} ranged from 30.9 to 129 μmol/L.[30] The other optimizations for these RyR1 agonists were equivalent to those of NSMPs. The sphere represented for the binding site contained the residues, which stayed within 9 Å from the residue, Gln4020-centered.

4.3.3. Protein—Ligand Interaction Prediction. Great efforts have been expended to explore the optimal binding modes between NSMPs and hRyR1, and molecular docking studies were carried out using the Libdock module in Discovery Studio 2.5 (Accelrys Software Inc., San Diego, CA, USA). Libdock is a docking program belonging to the semiflexible docking method, which has the characteristics of being rapid and accurate. There exist two rules for selecting the active compounds: (1) the docking scores must meet the threshold, that is, the Libdock score of the reference compound; (2) ligands must interact with at least three residues, which produced primary non-bond interactions during docking.

Discovery Studio Visualizer 2017 was utilized to observe the two-dimensional plots of interactions between a protein and a ligand and visualize the three-dimensional binding patterns.

4.4. Immunofluorescence Analysis. RTSMCs isolated were cultured on glass-bottom cell culture dishes according to the previous method.[70] The cells that were fixed for 10 min in ice-cold ethanol were washed two times in PBST. After being dehydrated with different volume fractions of ethanol and rinsed three times with PBS, the cells were then incubated with the antirabbit polyclonal antibody against α-SMA (1:50) overnight at 4 °C immediately after blocked with a normal goat serum working solution for 30 min. The cells were placed for 30 min at room temperature, then after being rinsed three times with PBS, they were incubated with the corresponding fluorescence-conjugated secondary antibodies (1:100) for 1 h at room temperature the following day. Following extensive rinsing, the images were captured using a laser confocal microscope (OLYMPUS FV100, Japan).

4.5. In Vitro Cell Viability Assay by the MTT Method. The cells, which were seeded at a density of 1.0×10^4 cells per well into 96-well plates, were cultured in DMEM with 10% FBS. After 1 day of serum starvation, the cells were incubated with eight concentrations of 10 NSMPs and 4-CmC (0.016, 0.16, 0.80, 1.6, 3.2, 8.0, 16, and 32 μM) for 2 h in DMEM with 2.0% FBS. After treatment, the cells were cultivated in MTT at 37 °C for 4 h immediately after the old medium was gotten rid of. Following the medium from each well discarded, the DMSO solution (150 μL/well) was added, vibrating for 10 min. Thereafter, when the formazan crystals had absolutely dissolved, the absorbance was read at a wavelength of 490 nm using a

microplate reader. All experiments were repeated in triplicate independently.

4.6. Measurement of $[Ca^{2+}]_{cyt}$ by Laser Confocal Microscopy. The cell density of rabbits tracheal smooth muscle cells (RTSMCs) was 8×10^4 cells/well. RTSMCs were randomly divided into two groups: the NSMP group and the NSMPs + ryanodine group. Each group was split into two subgroups: 0 μM and IC_{50} groups according to the concentration of NSMPs. After 1 day of serum starvation with DMEM containing 2.0% FBS, the cells were incubated with ryanodine at a final concentration of 10 μM for 15 min and then exposed to NSMPs at a final concentration of 0 μM and IC_{50}, respectively. After incubation with ryanodine and calcium ion indicators and Fluo-4 AM working solution for 15 min at 37 °C (Solarbio Biotechnology Co., Ltd., Beijing, China) with a final concentration of 5.0 μM, it was immediately washed three times with PBS. Finally, the changes in $[Ca^{2+}]_{cyt}$ were detected and analyzed by laser confocal microscopy.

4.7. Western Blotting Analysis. The cell density of RTSMCs seeded into 6-well plates was 2.0×10^5 cells per well. After 1 day of serum starvation with DMEM containing 2.0% FBS, the cells were exposed to 10 NSMPs and the reference compound for 24 h. Thereafter, the old medium of each well was discarded and the cells were rinsed with PBS, and then they were collected and lysed with RIPA buffer, shaking for 30 min at 4 °C. The cell lysis solution was gathered, respectively, and the protein concentration was quantified in accordance with the Bradford protein assay (BOSTER Biological Technology Co. Ltd., Wuhan, China). An equal amount of protein was transferred onto a polyvinylidene fluoride membrane, which was blocked in 5.0% non-fat milk, shaking at room temperature for 2 h immediately after electrophoresed in 10% SDS-PAGE. After that, it was cultivated with primary antibodies (RyR1, 1:1000; GAPDH, 1:10 000) overnight at 4 °C. On the following day, after being washed four times with TBST for 20 min, the blots were incubated in an antirabbit IgG horseradish peroxidase-conjugated secondary antibody for 1.5 h at room temperature. Finally, target proteins were further observed using the Western Lightning Chemiluminescence Reagent (PerkinElmer, USA) in a LabWorks gel imaging and analysis system. The target protein/GAPDH ratio was utilized to evaluate the relative expression of the target protein.

4.8. Statistical Analysis. All data were demonstrated as mean ± SD. Differences for multiple comparisons were evaluated using one-way or two-way analysis of variance (ANOVA) with GraphPad Prism 8.0 software. Among them, $P < 0.05$ was deemed statistically significant, while $P < 0.0001$ represented a high statistical difference.

■ ASSOCIATED CONTENT

⑤ Supporting Information

The Supporting Information is available free of charge at https://pubs.acs.org/doi/10.1021/acsomega.1c04468.

> Structural information of 132 NSMPs; docking modes between potential agonists of hRyR1 and hRyR1; effects of the positive small-molecule phenol 4-CmC and of potential NSMPs on the viability of RTSMCs with significant differences determined against the control group (PDF)

■ AUTHOR INFORMATION

Corresponding Author

Jianmei Huang − *School of Chinese Materia Medica, Beijing University of Chinese Medicine, Beijing 102488, China*; Email: huangjm@bucm.edu.cn

Authors

Yahong Chen − *School of Chinese Materia Medica, Beijing University of Chinese Medicine, Beijing 102488, China*; orcid.org/0000-0002-7473-4491

Xiaohong Wang − *School of Chinese Materia Medica, Beijing University of Chinese Medicine, Beijing 102488, China*

Haifeng Zhai − *National Institute on Drug Dependence, Peking University, Beijing 100191, China*

Yanling Zhang − *School of Chinese Materia Medica, Beijing University of Chinese Medicine, Beijing 102488, China*

Complete contact information is available at:
https://pubs.acs.org/10.1021/acsomega.1c04468

Author Contributions

Y.C. conceived and designed this work. X.W. collected and analyzed the data. H.Z., Y.Z., and J.H. revised the whole manuscript.

Notes

The authors declare no competing financial interest.

■ REFERENCES

(1) Ohayon, M. M. Anxiety disorders: Prevalence, comorbidity and outcomes. *J. Psychiatr. Res.* **2006**, *40*, 475−476.

(2) Nutt, D. J.; Ballenger, J. C.; Sheehan, D.; Wittchen, H.-U. Generalized anxiety disorder: comorbidity, comparative biology and treatment. *Int. J. Neuropsychopharmacol.* **2002**, *5*, 315−325.

(3) Sarris, J.; Kavanagh, D. J. Kava and St. John's Wort: current evidence for use in mood and anxiety disorders. *J. Altern. Complementary Med.* **2009**, *15*, 827.

(4) Pecknold, J. C.; Matas, M.; Howarth, B. G.; Ross, C.; Swinson, R.; Vezeau, C.; Ungar, W. Evaluation of buspirone as an antianxiety agent: buspirone and diazepam versus placebo. *Can. Psychiatr. Assoc. J.* **1989**, *34*, 766.

(5) Sarris, J.; Panossian, A.; Schweitzer, I.; Stough, C.; Scholey, A. Herbal medicine for depression, anxiety and insomnia: A review of psychopharmacology and clinical evidence. *Eur. Neuropsychopharmacol.* **2011**, *21*, 841−860.

(6) Wang, X.; Chen, Y.; Wang, Q.; Sun, L.; Li, G.; Zhang, C.; Huang, J.; Chen, L.; Zhai, H. Support for Natural Small-Molecule Phenols as Anxiolytics. *Molecules* **2017**, *22*, 2138.

(7) Vissiennon, C.; Nieber, K.; Kelber, O.; Butterweck, V. Route of administration determines the anxiolytic activity of the flavonols kaempferol, quercetin and myricetin−are they prodrugs? *J. Nutr. Biochem.* **2012**, *23*, 733−740.

(8) Mansouri, M. T.; Soltani, M.; Naghizadeh, B.; Farbood, Y.; Mashak, A.; Sarkaki, A. A possible mechanism for the anxiolytic-like effect of gallic acid in the rat elevated plus maze. *Pharmacol., Biochem. Behav.* **2014**, *117*, 40−46.

(9) Kwon, G.; Kim, H. J.; Park, S. J.; Lee, H. E.; Woo, H.; Ahn, Y. J.; Gao, Q.; Cheong, J. H.; Jang, D. S.; Ryu, J. H. Anxiolytic-like effect of danshensu [(3-(3,4-dihydroxyphenyl)-lactic acid)] in mice. *Life Sci.* **2014**, *101*, 73−78.

(10) Matsuura, Y.; Miyaichi, Y.; Tomimori, T. Studies on the Nepalese crude drugs. XIX. On the flavonoid and phenylethanoid constituents of the root of Scutellaria repens. *J. Pharm. Soc. Jpn.* **1994**, *114*, 775−788.

(11) Kohlmuenzer, S.; Chojnacka, W. E. Isolation of bergenin and some of its pharmacological properties. *Bull. Liaison—Groupe Polyphenols* **1986**, *13*, 590−593.

(12) Di, F.; Zhai, H.; Li, P.; Huang, J. Effects of dehydroeffusol on spasmogen-induced contractile responses of rat intestinal smooth muscles. *Planta Med.* **2014**, *80*, 978−983.

(13) Nagai, H.; He, J.-X.; Tani, T.; Akao, T. Antispasmodic activity of licochalcone A, a species-specific ingredient of Glycyrrhiza inflata roots. *J. Pharm. Pharmacol.* **2007**, *59*, 1421−1426.

(14) Mustafa, M. R.; Mohamad, R.; Din, L.; Wahid, S. Smooth muscle relaxant activities of compounds isolated from malaysian medicinal plants on rat aorta and guinea-pig ileum. *Phytother. Res.* **1995**, *9*, 555−558.

(15) Babbar, N.; Oberoi, H. S.; Sandhu, S. K.; Bhargav, V. K. Influence of different solvents in extraction of phenolic compounds from vegetable residues and their evaluation as natural sources of antioxidants. *J. Food Sci. Technol.* **2014**, *51*, 2568−2575.

(16) Stefani, M.; Rigacci, S. Beneficial properties of natural phenols: highlight on protection against pathological conditions associated with amyloid aggregation. *Biofactors* **2014**, *40*, 482−493.

(17) Jurd, L.; King, A. D., Jr.; Mihara, K.; Stanley, W. L. Antimicrobial properties of natural phenols and related compounds. *Appl. Microbiol.* **1971**, *21*, 507−510.

(18) Kimlicka, L.; Van Petegem, F. The structural biology of ryanodine receptors. *Sci. China: Life Sci.* **2011**, *54*, 712−724.

(19) Van Petegem, F. Ryanodine receptors: allosteric ion channel giants. *J. Mol. Biol.* **2015**, *427*, 31−53.

(20) Van Petegem, F. Ryanodine receptors: structure and function. *J. Biol. Chem.* **2012**, *287*, 31624−31632.

(21) Bai, X.-C.; Yan, Z.; Wu, J.; Li, Z.; Yan, N. The Central domain of RyR1 is the transducer for long-range allosteric gating of channel opening. *Cell Res.* **2016**, *26*, 995−1006.

(22) Zucchi, R.; Ronca-Testoni, S. The sarcoplasmic reticulum Ca2+ channel/ryanodine receptor: modulation by endogenous effectors, drugs and disease states. *Pharmacol. Rev.* **1997**, *49*, 1.

(23) Herrmann-Frank, A.; Richter, M.; Sarközi, S.; Mohr, U.; Lehmann-Horn, F. 4-Chloro-m-cresol, a potent and specific activator of the skeletal muscle ryanodine receptor. *Biochim. Biophys. Acta, Gen. Subj.* **1996**, *1289*, 31−40.

(24) Fessenden, J. D.; Feng, W.; Pessah, I. N.; Allen, P. D. Amino acid residues Gln4020 and Lys4021 of the ryanodine receptor type 1 are required for activation by 4-chloro-m-cresol. *J. Biol. Chem.* **2006**, *281*, 21022−21031.

(25) Szentesi, P.; Szappanos, H.; Szegedi, C.; Gönczi, M.; Jona, I.; Cseri, J.; Kovács, L.; Csernoch, L. Altered elementary calcium release events and enhanced calcium release by thymol in rat skeletal muscle. *Biophys. J.* **2004**, *86*, 1436−1453.

(26) Sárközi, S.; Almássy, J.; Lukács, B.; Dobrosi, N.; Nagy, G.; Jóna, I. Effect of natural phenol derivatives on skeletal type sarcoplasmic reticulum Ca2+ -ATPase and ryanodine receptor. *J. Muscle Res. Cell Motil.* **2007**, *28*, 167−174.

(27) Lee, E. H.; Meissner, G.; Kim, D. H. Effects of quercetin on single Ca(2+) release channel behavior of skeletal muscle. *Biophys. J.* **2002**, *82*, 1266−1277.

(28) Young, R.; Glennon, R. A. Discriminative stimulus properties of amphetamine and structurally related phenalkylamines. *Med. Res. Rev.* **1986**, *6*, 99−130.

(29) Capela, J. P.; Carmo, H.; Remião, F.; Bastos, M. L.; Meisel, A.; Carvalho, F. Molecular and cellular mechanisms of ecstasy-induced neurotoxicity: an overview. *Mol. Neurobiol.* **2009**, *39*, 210−271.

(30) Jacobson, A. R.; Moe, S. T.; Allen, P. D.; Fessenden, J. D. Structural determinants of 4-chloro-m-cresol required for activation of ryanodine receptor type 1. *Mol. Pharmacol.* **2006**, *70*, 259−266.

(31) Kumar, V. Potential medicinal plants for CNS disorders: an overview. *Phytother. Res.* **2006**, *20*, 1023−1035.

(32) Wang, X.; Li, G.; Li, P.; Huang, L.; Huang, J.; Zhai, H. Anxiolytic effects of orcinol glucoside and orcinol monohydrate in mice. *Pharm. Biol.* **2015**, *53*, 876−881.

(33) Ren, L.; Wang, F.; Xu, Z.; Chan, W. M.; Zhao, C.; Xue, H. GABA(A) receptor subtype selectivity underlying anxiolytic effect of 6-hydroxyflavone. *Biochem. Pharmacol.* **2010**, *79*, 1337−1344.

(34) Wolfman, C.; Viola, H.; Paladini, A.; Dajas, F.; Medina, J. H. Possible anxiolytic effects of chrysin, a central benzodiazepine receptor ligand isolated from Passiflora coerulea. *Pharmacol., Biochem. Behav.* **1994**, *47*, 1−4.

(35) Viola, H.; Wasowski, C.; Levi de Stein, M.; Wolfman, C.; Silveira, R.; Dajas, F.; Medina, J. H.; Paladini, A. C. Apigenin, a component of Matricaria recutita flowers, is a central benzodiazepine receptors-ligand with anxiolytic effects. *Planta Med.* **1995**, *61*, 213−216.

(36) de Carvalho, R. S. M.; Duarte, F. S.; de Lima, T. C. M. Involvement of GABAergic non-benzodiazepine sites in the anxiolytic-like and sedative effects of the flavonoid baicalein in mice. *Behav. Brain Res.* **2011**, *221*, 75−82.

(37) Raines, T.; Jones, P.; Moe, N.; Duncan, R.; McCall, S.; Ceremuga, T. E. Investigation of the anxiolytic effects of luteolin, a lemon balm flavonoid in the male Sprague-Dawley rat. *J. Am. Assoc. Nurse Anesth.* **2009**, *77*, 33−36.

(38) Marder, M.; Viola, H.; Wasowski, C.; Fernández, S.; Medina, J. H.; Paladini, A. C. 6-methylapigenin and hesperidin: new valeriana flavonoids with activity on the CNS. *Pharmacol., Biochem. Behav.* **2003**, *75*, 537−545.

(39) Hui, K. M.; Huen, M. S. Y.; Wang, H. Y.; Zheng, H.; Sigel, E.; Baur, R.; Ren, H.; Li, Z. W.; Wong, J. T.-F.; Xue, H. Anxiolytic effect of wogonin, a benzodiazepine receptor ligand isolated from Scutellaria baicalensis Georgi. *Biochem. Pharmacol.* **2002**, *64*, 1415−1424.

(40) Mangaiarkkarasi, A.; Viswanathan, S.; Ramaswamy, S.; Tharani, C. B. Anxiolytic effect of Morin in mice. *Int. J. Life Sci. Pharma Res.* **2012**, *2*, 52−60.

(41) Kushnir, A.; Marks, A. R. The ryanodine receptor in cardiac physiology and disease. *Adv. Pharmacol.* **2010**, *59*, 1−30.

(42) Endo, M. Calcium-induced calcium release in skeletal muscle. *Physiol. Rev.* **2009**, *89*, 1153−1176.

(43) Fan, J.; Jin, Y.; Xin, Z.; Dong, Z.; Wang, L.; Xu, M. M.; Mu, Y.; Nishi, M.; Isaacs, W.; An, S. Ryanodine Receptors: Functional Structure and Their Regulatory Factors. *Chin. J. Cell Bio.* **2015**, *37*, 6−15.

(44) Annaházi, A.; Roka, R.; Rosztoczy, A.; Wittmann, T. Role of antispasmodics in the treatment of irritable bowel syndrome. *World J. Gastroenterol.* **2014**, *20*, 6031−6043.

(45) Oztekin, Ç. V.; Gur, S.; Abdulkadir, N. A.; Kartal, M.; Karabakan, M.; Akdemir, A. O.; Gökkaya, C. S.; Cetinkaya, M. Analysis of pomegranate juice components in rat corpora cavernosal relaxation. *Int. J. Impotence Res.* **2014**, *26*, 45−50.

(46) Ponce-Monter, H.; Perez, S.; Zavala, M. A.; Perez, C.; Meckes, M.; Macias, A.; Campos, M. Relaxant effect of xanthomicrol and 3alpha-angeloyloxy-2alpha-hydroxy-13,14z-dehydrocativic acid from Brickellia paniculata on rat uterus. *Biol. Pharm. Bull.* **2006**, *29*, 1501−1503.

(47) Leal, L. K. A. M.; Costa, M. F.; Pitombeira, M.; Barroso, V. M.; Silveira, E. R.; Canuto, K. M.; Viana, G. S. B. Mechanisms underlying the relaxation induced by isokaempferide from Amburana cearensis in the guinea-pig isolated trachea. *Life Sci.* **2006**, *79*, 98−104.

(48) Campos, M. G.; Oropeza, M. V.; Villanueva, T.; Aguilar, M. I.; Delgado, G.; Ponce, H. A. Xanthorrhizol induces endothelium-independent relaxation of rat thoracic aorta. *Life Sci.* **2000**, *67*, 327−333.

(49) Mustafa, E. H.; Abu Zarga, M.; Abdalla, S. Effects of cirsiliol, a flavone isolated from Achillea fragrantissima, on rat isolated ileum. *Gen. Pharmacol.* **1992**, *23*, 555−560.

(50) Ye, Y.; Yaeger, D.; Owen, L. J.; Escobedo, J. O.; Wang, J.; Singer, J. D.; Strongin, R. M.; Abramson, J. J. Designing calcium release channel inhibitors with enhanced electron donor properties: stabilizing the closed state of ryanodine receptor type 1. *Mol. Pharmacol.* **2012**, *81*, 53−62.

(51) Marinov, B. S.; Olojo, R. O.; Xia, R.; Abramson, J. J. Non-thiol reagents regulate ryanodine receptor function by redox interactions that modify reactive thiols. *Antioxid. Redox Signaling* **2007**, *9*, 609−621.

(52) Zorzato, F.; Scutari, E.; Tegazzin, V.; Clementi, E.; Treves, S. Chlorocresol: an activator of ryanodine receptor-mediated Ca^{2+} release. *Mol. Pharmacol.* **1993**, *44*, 1192−1201.

(53) Gordienko, D. V.; Bolton, T. B. Crosstalk between ryanodine receptors and IP(3) receptors as a factor shaping spontaneous $Ca^{(2+)}$-release events in rabbit portal vein myocytes. *J. Physiol.* **2002**, *542*, 743−762.

(54) Ouedraogo, N.; Roux, E.; Forestier, F.; Rossetti, M.; Savineau, J.-P.; Marthan, R. Effects of intravenous anesthetics on normal and passively sensitized human isolated airway smooth muscle. *Anesthesiology* **1998**, *88*, 317−326.

(55) Kwon, G.; Kim, H. J.; Park, S. J.; Lee, H. E.; Woo, H.; Ahn, Y. J.; gao, Q.; Cheong, J. H.; Jang, D. S.; Ryu, J. H. Anxiolytic-like effect of danshensu [(3-(3,4-dihydroxyphenyl)-lactic acid)] in mice. *Life Sci.* **2014**, *101*, 73−78.

(56) Takeda, H.; Tsuji, M.; Miyamoto, J.; Masuya, J.; Iimori, M.; Matsumiya, T. Caffeic acid produces antidepressive- and/or anxiolytic-like effects through indirect modulation of the alpha 1A-adrenoceptor system in mice. *NeuroReport* **2003**, *14*, 1067−1070.

(57) Scheepens, A.; Bisson, J.-F.; Skinner, M. p-Coumaric Acid Activates the GABA-A Receptor In Vitro and is Orally Anxiolytic In Vivo. *Phytother. Res.* **2014**, *28*, 207−211.

(58) Jung, J. W.; Yoon, B. H.; Oh, H. R.; Ahn, J.-H.; Kim, S. Y.; Park, S.-Y.; Ryu, J. H. Anxiolytic-like effects of Gastrodia elata and its phenolic constituents in mice. *Biol. Pharm. Bull.* **2006**, *29*, 261−265.

(59) Radermacher, M.; Rao, V.; Grassucci, R.; Frank, J.; Timerman, A. P.; Fleischer, S.; Wagenknecht, T. Cryo-electron microscopy and three-dimensional reconstruction of the calcium release channel/ryanodine receptor from skeletal muscle. *J. Cell Biol.* **1994**, *127*, 411−423.

(60) Aguirre-Hernández, E.; González-Trujano, M. E.; Martínez, A. L.; Moreno, J.; Kite, G.; Terrazas, T.; Soto-Hernández, M. HPLC/MS analysis and anxiolytic-like effect of quercetin and kaempferol flavonoids from Tilia americana var. mexicana. *J. Ethnopharmacol.* **2010**, *127*, 91−97.

(61) Pine, A.; Shiner, T.; Seymour, B.; Dolan, R. J. Dopamine, time, and impulsivity in humans. *J. Neurosci.* **2010**, *30*, 8888−8896.

(62) Anderson, W.; Barrows, M.; Lopez, F.; Rogers, S.; Ortiz-Coffie, A.; Norman, D.; Hodges, J.; McDonald, K.; Barnes, D.; McCall, S.; Don, J. A.; Ceremuga, T. E. Investigation of the anxiolytic effects of naringenin, a component of Mentha aquatica, in the male Sprague-Dawley rat. *Holist. Nurs. Pract.* **2012**, *26*, 52−57.

(63) Stringer, T. P.; Guerrieri, D.; Vivar, C.; van Praag, H. Plant-derived flavanol (-)epicatechin mitigates anxiety in association with elevated hippocampal monoamine and BDNF levels, but does not influence pattern separation in mice. *Transl. Psychiatry* **2015**, *5*, No. e493.

(64) Young, R.; Glennon, R. A. Discriminative stimulus properties of amphetamine and structurally related phenalkylamines. *Med. Res. Rev.* **1986**, *6*, 99−130.

(65) Klein, M. O.; Battagello, D. S.; Cardoso, A. R.; Hauser, D. N.; Bittencourt, J. C.; Correa, R. G. Dopamine: Functions, Signaling, and Association with Neurological Diseases. *Cell. Mol. Neurobiol.* **2019**, *39*, 31−59.

(66) Zucca, F. A.; Segura-Aguilar, J.; Ferrari, E.; Muñoz, P.; Paris, I.; Sulzer, D.; Sarna, T.; Casella, L.; Zecca, L. Interactions of iron, dopamine and neuromelanin pathways in brain aging and Parkinson's disease. *Prog. Neurobiol.* **2017**, *155*, 96−119.

(67) Grace, A. A.; Gomes, F. V. The Circuitry of Dopamine System Regulation and its Disruption in Schizophrenia: Insights Into Treatment and Prevention. *Schizophr. Bull.* **2019**, *45*, 148−157.

(68) Wang, X.; Zhang, Y.; Liu, Q.; Ai, Z.; Zhang, Y.; Xiang, Y.; Qiao, Y. Discovery of Dual ETA/ETB Receptor Antagonists from Traditional Chinese Herbs through in Silico and in Vitro Screening. *Int. J. Mol. Sci.* **2016**, *17*, 389.

(69) Wei, R.; Wang, X.; Zhang, Y.; Mukherjee, S.; Zhang, L.; Chen, Q.; Huang, X.; Jing, S.; Liu, C.; Li, S.; Wang, G.; Xu, Y.; Zhu, S.; Williams, A.

J.; Sun, F.; Yin, C.-C. Structural insights into Ca(2+)-activated long-range allosteric channel gating of RyR1. *Cell Res.* **2016**, *26*, 977−994.

(70) Hardingham, G. E.; Chawla, S.; Johnson, C. M.; Bading, H. Distinct functions of nuclear and cytoplasmic calcium in the control of gene expression. *Nature* **1997**, *385*, 260−265.